

# HOT ROLLING OF THE SUPERAUSTENITIC STAINLESS STEEL AISI 904L

## VROČE VALJANJE SUPERAVSTENITNEGA NERJAVNEGA JEKLA AIS I 904L

**Franc Tehovnik, Borut Žužek, Boštjan Arh, Jaka Burja, Bojan Podgornik**

Institute of Metals and Technology, Lepi pot 11, 1000 Ljubljana, Slovenia  
franc.tehovnik@imt.si

*Prejem rokopisa – received: 2013-11-04; sprejem za objavo – accepted for publication: 2013-12-06*

The AISI 904L superaustenitic stainless steel has a narrow processing window. In this work the hot rolling of steel, specifically the hot deformation behavior, is investigated. Specimens of steel were hot rolled at temperatures from 1000 °C to 1250 °C with 50 °C increments and the rolling loads were measured and recorded. Microstructural changes were examined, with the accent on the recrystallization. From changes of the hot-rolling loads and microstructure it is concluded that the recrystallization begins at temperatures around 1050 °C and three passes of 20 % deformation at the deformation rate of 5 s<sup>-1</sup>. In order to avoid over loads of rolling stand at equal deformation rate and degree, the recommended temperature was 1100 °C. The upper hot-working temperatures were not as clearly determined, it is considered to be around 1250 °C.

Keywords: hot rolling, superaustenitic stainless steel, microstructure evolution, segregation bands

Superavstenitno nerjavno jeklo AISI 904L ima ozko temperaturno območje vročega preoblikovanja. V tem delu je preiskovano vroče valjanje oziroma vedenje jekla med vročim preoblikovanjem. Vzorci jekla so bili valjani pri temperaturah med 1000 °C in 1250 °C s koraki po 50 °C in izmerjene ter zabeležene so bile sile valjanja. Preiskovane so bile spremembe mikrostrukture s poudarkom na rekristalizaciji. Iz spremembe velikosti sil vročega preoblikovanja in mikrostrukturnih sprememb je bilo ugotovljeno, da se rekristalizacija začne pri temperaturi okoli 1050 °C po treh prevlekih z 20 % deformacijo in pri hitrosti deformacije okoli 5 s<sup>-1</sup>. Zaradi izogibanja velikim obremenitvam valjavskega ogrođja je spodnja priporočljiva meja preoblikovanja pri tej hitrosti deformacije postavljena pri 1100 °C. Za zgornjo mejo procesnega okna je bila predlagana temperatura okrog 1250 °C.

Ključne besede: vroče valjanje, superavstenitno nerjavno jeklo, razvoj mikrostrukture, segregacija

## 1 INTRODUCTION

The high-alloyed austenitic grades of stainless steels exhibit greater corrosion resistance and higher strength compared with standard stainless steel grades, e.g., ferritic or austenitic grades.<sup>1</sup> Compared to standard austenitic stainless steels, superaustenitic stainless steels have a similar microstructure, but a higher content of some elements, such as chromium, nickel, molybdenum, copper and nitrogen, that increase the strength and corrosion resistance. As the content of alloying elements increases, problems of industrial processing become more severe. The high-temperature strength increases and the softening rate is minimal at temperatures below 950 °C.<sup>2</sup>

To avoid excessive mill loading, hot working is often carried out at a high rolling temperature.<sup>3</sup> The presence of some alloying elements, e.g., molybdenum, has a negative influence on the hot ductility of austenitic steels.<sup>4</sup> Upper hot working temperatures are limited, because of the hot shortness, which results from segregation of alloying elements during casting.<sup>5,6</sup> Segregations at grain boundaries melt at high temperatures and the steel cracks during hot working. However, when properly heated, segregation-rich bands are elongated by hot rolling. The brittle sigma phase, which is the most common intermetallic precipitate in austenitic stainless

steels,<sup>7</sup> precipitates within these bands and affects the mechanical properties.<sup>8,9</sup> Therefore, the processing window of superaustenitic steels is quite narrow, often just 150–200 °C and is related to a series of complex processes taking place during deformation.<sup>10</sup> Austenite has a low stacking-fault energy (SFE) and both dynamic recrystallization (DRX) and static recrystallization (SRX) play an important role in the evolution of the microstructure during and after hot deformation.<sup>11</sup> It was frequently reported that DRX is the dominant restoration mechanism during the hot deformation of austenitic stainless steels.<sup>12–15</sup> DRX depends on the processing temperature and deformation rate.<sup>16,17</sup>

The present work is aimed at investigating a part of the complex processes that take place in the narrow processing window of AISI 904L, an industrially important superaustenitic stainless steel.

## 2 EXPERIMENTAL

For hot-rolling tests, flat specimens of AISI 904L, with the chemical composition in **Table 1**, were used. The specimens were cut from a thick hot-rolled plate 20 mm and had a length of 145 mm and a width of 46 mm. The soaking temperatures were (1000, 1050, 1100, 1150, 1200 and 1250) °C, the soaking time was 30 min. The deformation per pass was 20 % and three passes were

**Table 1:** Chemical composition of AISI 904L in mass fractions (w/%)**Tabela 1:** Kemijska sestava AISI 904L v masnih deležih (w/%)

Chemical composition (w/%)									
C	Si	Mn	P	S	Cr	Ni	Mo	Cu	N
0.006	0.22	1.41	0.019	0.0005	19.61	26.1	3.9	1.4	0.0686

made for each specimen. The deformation rate during rolling was calculated to be  $5 \text{ s}^{-1}$ . The rolled specimens were then air cooled and prepared for light microscopy (LOM) examinations. The rolling loads were measured with a measurement system with 2000 recordings per second. A specimen with an initial microstructure was isothermally annealed at  $950 \text{ }^\circ\text{C}$  for 30 min and examined with light and electron microscopy.

### 3 RESULTS AND DISCUSSION

**Figure 1** shows the initial microstructure of AISI 904L. The initial grain size was  $110 \text{ }\mu\text{m}$ , with a large number of annealing twins in austenite grains typical for alloys with a low SFE<sup>13</sup>.

The rolling loads measured at six different temperatures during three passes are shown in **Figure 2**. The loads decrease with an increasing temperature. The rolling loads at  $1000 \text{ }^\circ\text{C}$  are the highest, and in the range from  $1100 \text{ kN}$  to  $1300 \text{ kN}$ . The loads at  $1250 \text{ }^\circ\text{C}$  are the lowest, and increase from about  $500 \text{ kN}$  measured during the first pass to over  $800 \text{ kN}$  in the third pass. The average load rises with each pass, which can be attributed to the fall of temperature in the rolling specimen and to incomplete DRX. It is supposed that the peaks in load at the start or the end of the pass (**Figure 2**) are the result of temperature differences due faster cooling at the specimens' edges.

While the edged surfaces of the measurements of loads at lower temperatures  $1000 \text{ }^\circ\text{C}$  to  $1100 \text{ }^\circ\text{C}$  are attributed to the measurement system, the problem becomes more serious at higher loads. The most drastic change in

load was observed after the second pass at  $1100 \text{ }^\circ\text{C}$ . Based on the jump of the load it is evident that the temperature of hot deformation for this steel should not be lower than  $1100 \text{ }^\circ\text{C}$ . Therefore, it can be concluded that the lower temperature of the processing window at the deformation rate of  $5 \text{ s}^{-1}$  is  $1100 \text{ }^\circ\text{C}$ . The LOM analysis of the microstructure confirmed a significant change at  $1100 \text{ }^\circ\text{C}$ , where the DRX becomes most evident (**Figure 3**).

The austenite microstructure obtained after hot rolling with  $3 \times 20 \%$  deformation at different temperature is shown in **Figure 3**. The serrated boundaries of highly elongated grains and local bulges are clearly observed in the microstructure with a rolling temperature of  $1050 \text{ }^\circ\text{C}$  (**Figure 3b**). The initial stages of DRX appear on the grain boundaries.

The first recrystallized grains were visible after rolling at  $1050 \text{ }^\circ\text{C}$ . The extent of the recrystallization increased with temperature and was  $100 \%$  at  $1200 \text{ }^\circ\text{C}$ . The changes of microstructure show that the most significant rise of DRX occurs at  $1150 \text{ }^\circ\text{C}$ , as shown by a comparison of **Figures 3c** and **3d**. In both cases the existence of equiaxed grains confirms the occurrence of DRX already during the hot rolling. The presence of deformed austenite grains are a clear sign of incomplete DRX. The recrystallization process here includes distinct nucleation and growth stages of new grains at the interface of the recrystallized and non-recrystallized regions.<sup>12–14</sup> This process goes on until all the stored energy is used.<sup>18</sup> Once DRX is completed, the steady state is established as a result of a dynamic balance

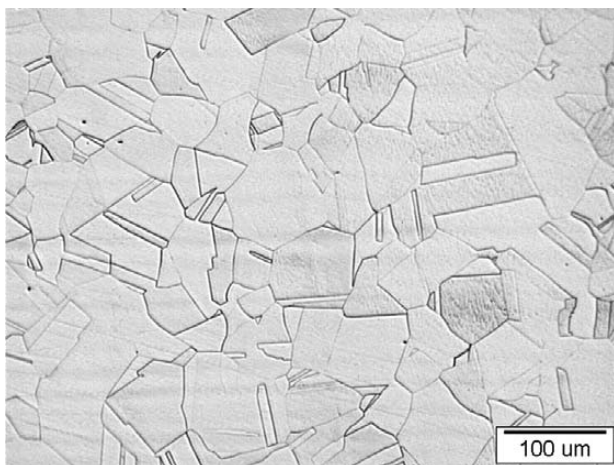


**Figure 1:** Initial steel microstructure after solution annealing  
**Slika 1:** Začetna mikrostruktura jekla po raztopnem žarjenju

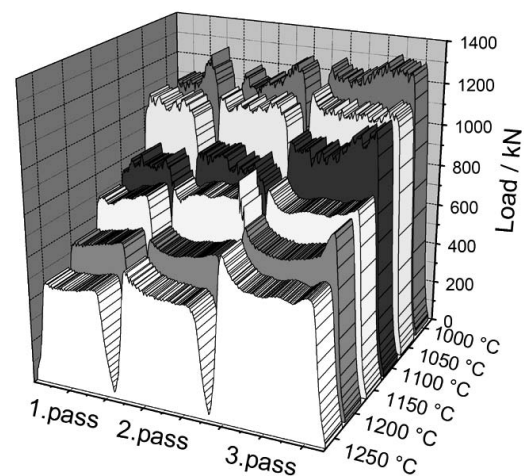


**Figure 2:** Rolling load per pass at different temperatures during hot rolling

**Slika 2:** Sile valjanja pri posameznem prevleku pri različnih temperaturah vročega valjanja

between recrystallization and work hardening.<sup>16-18</sup> There are no recrystallized grains in the samples rolled at 1000 °C, which indicates that no DRX has taken place. An apparently fully dynamically recrystallized microstructure is present at 1200 °C and 1250 °C and at this temperature a greater grain growth than at 1200 °C is observed. Therefore, 1250 °C is supposed to be the upper processing temperature for a fine-grained microstructure. The presence of a few twin boundaries is also found in the DRX grains. These newly formed twin boundaries are reported to be active nucleation sites for continuing DRX during straining<sup>13</sup>.

As shown in **Figures 3b** and **3c**, recrystallization nuclei appear on the grain and twin boundaries, thus confirming the necklace DRX mechanism. The new recrystallized grains nucleate on the deformed grain boundaries and form a necklace around it.<sup>18-20</sup>

The segregation of alloying elements occurs during the solidification of AISI 904L. The sigma phase ( $\sigma$ -phase) forms from the austenite, because the solidification is primarily austenitic for all austenitic stainless steels with the  $w(\text{Cr}_{\text{eq}})/w(\text{Ni}_{\text{eq}}) < 1.5$ <sup>21</sup>, AISI 904L  $w(\text{Cr}_{\text{eq}})/w(\text{Ni}_{\text{eq}}) = 0.9$  and in interdendritic areas the contents of chromium and molybdenum are increased. **Figure 4** shows the  $\sigma$ -phase precipitates also within austenite grains as a consequence of segregations. During rolling the segregations are elongated and are observed as dark bands in etched metallographic

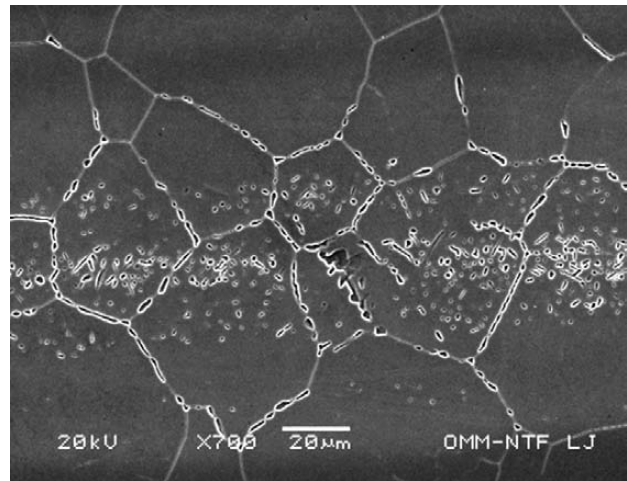


**Figure 4:**  $\sigma$ -phase precipitates at 950 °C  
**Slika 4:** Izločanje  $\sigma$ -faze pri 950 °C

samples. An EDS analysis did not reveal a greater change in the concentration of the alloying elements because the area of sampling is too large. But after isothermal annealing at 950 °C larger  $\sigma$ -phase precipitates can be observed (**Figure 4**), confirming the existence of the segregations.

Dendrite segregations occur because of the high content of chromium and molybdenum and are possible because the ratio between the ferrite and austenite

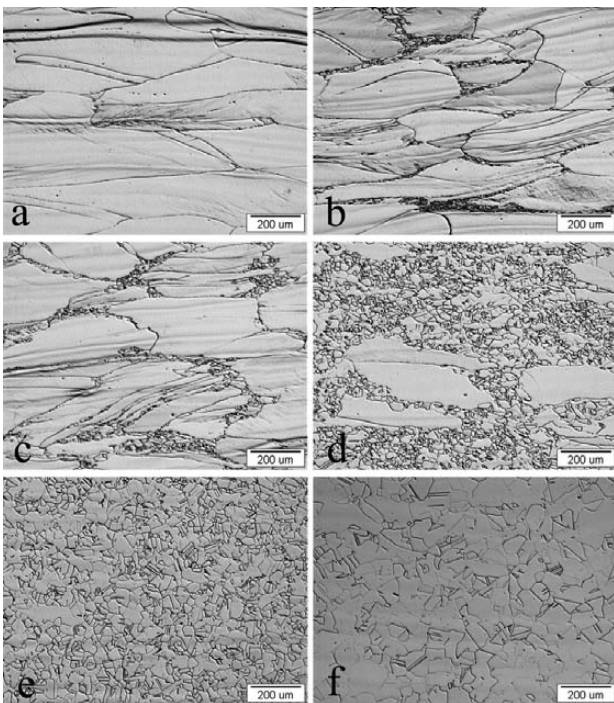


**Figure 3:** Microstructure of specimens after three rolling passes at different temperatures: a) 1000 °C, b) 1050 °C, c) 1100 °C, d) 1150 °C, e) 1200 °C, f) 1250 °C

**Slika 3:** Mikrostruktura vzorcev po treh prevlekih pri različnih temperaturah valjanja: a) 1000 °C, b) 1050 °C, c) 1100 °C, d) 1150 °C, e) 1200 °C, f) 1250 °C

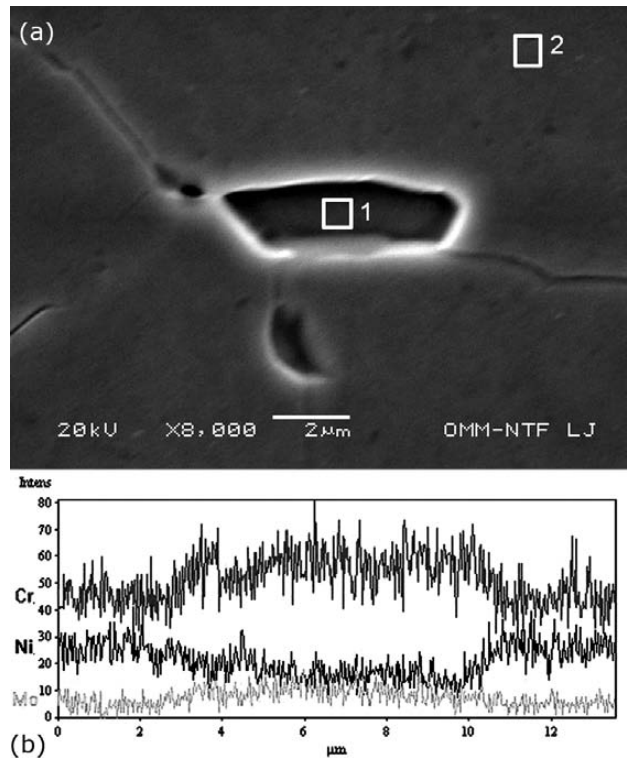


**Figure 5:** SEM image of  $\sigma$ -precipitate with marked points of EDS analysis, b) line scan analysis across  $\sigma$ -phase precipitate

**Slika 5:** a) SEM-posnetek izločka  $\sigma$ -faze z označenimi mesti EDS analiz, b) linijska analiza porazdelitve elementov preko  $\sigma$ -fazi

forming elements changed in the austenite grains. At 950 °C  $\sigma$ -phase precipitates at the grain boundaries and in the segregation band in the form of lamellas or irregular shapes. The chromium contents in the  $\sigma$ -phase can reach up to 30 %, molybdenum contents are from 15 % to 20 %, nickel contents are below 14 %, as can be seen in the EDS analysis of the  $\sigma$ -phase in **Figure 5**, the results of the analysis are given in **Table 2**. Alloying elements, such as chromium, molybdenum and silicon, promote the formation of the  $\sigma$ -phase, while nickel and nitrogen retard it. The  $\sigma$ -phase mostly forms at the austenite grain boundaries, triple junctions and incoherent twin borders.

A line scan of a spheridised  $\sigma$ -phase on the austenite grain boundaries shows higher contents of chromium and molybden and lower contents of nickel. The line scan is shown in **Figure 5**.

**Table 2:** Chemical composition of  $\sigma$ -phase and matrix from **Figure 5**  
**Tabela 2:** Kemijska sestava  $\sigma$ -faze in matrice s **slike 5**

Chemical composition (w/%)							
Spectrum	Si	Mn	Cr	Ni	Mo	Cu	Fe
1	0.54	1.26	30.47	10.70	19.02	0.00	38.00
2	0.27	1.52	19.92	22.99	4.75	2.55	48.00

## 4 CONCLUSIONS

The microstructure of the superaustenitic stainless steel AISI 904L after hot rolling consists only of austenite. With three 20 % rolling passes with a deformation rate of 5 s<sup>-1</sup> the first recrystallized grains appear at the rolling temperature of 1050 °C and the degree of recrystallization increases with higher temperatures. Recrystallization nuclei were found to form on the grain boundaries, triple junctions and at incoherent twin boundaries. The newly formed recrystallized grains form the so-called "necklace" recrystallization mechanism as a clear sign of DRX. Across the segregation areas with high chromium and molybdenum contents the  $\sigma$ -phase precipitates intragranularly and intergranularly.

## Acknowledgment

The authors would like to thank ACRONI Jesenice for financial support; the work was part of an industrial project. We would especially like to thank Mr. Boštjan Pirnar, M. Sc. from ACRONI for his part in the project.

## 5 REFERENCES

- L. Tan, K. Sridharan, T. R. Allen, R. K. Nanstad, D. A. McClintock, Microstructure tailoring for property improvements by grain boundary engineering, *J. Nucl. Mater.*, 374 (2008), 270–280
- B. Bradaškja, B. Pirnar, M. Fazarinc, P. Fajfar, Deformation Behaviour and Microstructural Evolution During Hot Compression of AISI 904L, *Steel Res. Int.*, 82 (2011) 4, 346–351
- M. Mukherjee, T. Pal, Role of microstructural constituents on surface crack formation during hot rolling of standard and low nickel austenitic stainless steels, *Acta Metall. Sin. (Engl. Lett.)*, 26 (2013), 206–216
- F. Tehovnik, D. Steiner Petrovič, F. Vode, J. Burja, Influence of Molybdenum on The Hot-Tensile Properties of Austenitic Stainless Steels, *Mater. Tehnol.*, 46 (2012) 6, 649–655
- F. Tehovnik, F. Vodopivec, B. Arzenšek, R. Celin, The effect of lead on the hot workability of austenitic stainless steel with a solidification structure, *Metalurgija*, 49 (2010), 49–52
- M. Torkar, Effect of Trace and Residual Elements on The Hot Brittleness, Hot Shortness and Properties of 0.15–0.3 % C Al-Killed Steels with a Solidification Microstructure, *Mater. Tehnol.*, 44 (2010) 6, 327–333
- M. Vach et al., Evolution of secondary phases in austenitic stainless steels during long-term exposures at 600, 650 and 800 °C, *Mater. Charact.*, 59 (2008), 1792–1798
- R. W. Fonda, E. M. Lauridsen, W. Ludwig, P. Tafforeau, G. Spanos, Two-Dimensional and Three-Dimensional Analyses of Sigma Precipitates and Porosity in a Superaustenitic Stainless Steel, *Metall. Mater. Trans. A*, 38 (2007), 2721–2726
- A. C. Stauffer, D. A. Koss, J. B. Mckirgan, Microstructural Banding and Failure of a Stainless Steel, *Metall. Mater. Trans. A*, 35A (2004), 1317–1327
- R. M. Forbes Jones, L. A. Jackman, The structural evolution of superalloy ingots during hot working, *JOM*, 51 (1999), 27–31
- A. Belyakov, H. Miura, T. Sakai, Dynamic recrystallization in ultra fine-grained 304 stainless steel, *Scr. Mater.*, 43 (2000), 21–26
- A. Momeni, K. Dehghani, H. Keshmiri, G. R. Ebrahimi, Hot deformation behavior and microstructural evolution of a superaustenitic stainless steel, *Mater. Sci. Eng. A*, 527 (2010), 1605–1611
- A. Hoseini Asli, A. Zarei-Hanzaki, Dynamic Recrystallization Behavior of a Fe-Cr-Ni Super-Austenitic Stainless Steel, *J. Mater. Sci. Technol.*, 25 (2009), 603–606
- R. Puli, G. D. Janaki Ram, Dynamic recrystallization in friction surfaced austenitic stainless steel coatings, *Mater. Charact.*, 74 (2012), 49–54
- P. Fajfar, B. Bradaškja, B. Pirnar, M. Fazarinc, Determination of hot workability and processing maps for AISI 904L stainless steel, *RMZ – Materials and Geoenvironment*, 58 (2011), 383–91
- M. Tikhonova, R. Kaibyshev, X. Fang, W. Wang, A. Belyakov, Grain boundary assembles developed in an austenitic stainless steel during large strain warm working, *Mater. Charact.*, 70 (2012), 14–20
- Z. Yanushkevich, A. Mogucheva, M. Tikhonova, A. Belyakov, R. Kaibyshev, Structural strengthening of an austenitic stainless steel subjected to warm-to-hot working, *Mater. Charact.*, 62 (2011), 432–437
- A. Momeni, K. Dehghani, Microstructural Evolution and Flow Analysis during Hot Working of a Fe-Ni-Cr Superaustenitic Stainless Steel, *Metall. Mater. Trans. A*, 42 (2010), 1925–1932
- H. Mirzadeh, A. Najafizadeh, Hot Deformation and Dynamic Recrystallization of 17-4 PH Stainless Steel, *ISIJ Int.*, 53 (2013), 680–689
- Y. Han, G. Liu, D. Zou, R. Liu, G. Qiao, Deformation behavior and microstructural evolution of as-cast 904L austenitic stainless steel during hot compression, *Mater. Sci. Eng. A*, 565 (2013), 342–350
- N. Suutala, Effect of solidification conditions on the solidification mode in austenitic stainless steels, *Metall. Trans. A*, 14A (1983), 191–197